Modal Approximation of Distributed Dynamics for a Hydraulic Transmission Line With Pressure Input-Flow Rate Output Causality

Beshahwired Ayalew
e-mail: beshah@psu.edu

Bohdan T. Kulakowski
e-mail: btk1@psu.edu

The Pennsylvania State University, 201 Transportation Research Building, University Park, PA 16802

Based on analytical results obtained in the frequency domain, modal approximation techniques are employed to derive transfer function and state space models applicable to a pressure input-flow rate output causality case of a transmission line. The causality case considered here arises while modeling short connection lines to hydraulic accumulators. However, the modal approximation results presented apply also to other cases where the linear friction model is considered applicable. It is highlighted that the results presented can reduce the overall order of the hydraulic system model containing the transmission line being considered.

[DOI: 10.1115/1.1978913]

1 Introduction

For the study of hydraulic fluid transients in transmission lines, various modeling techniques have been proposed [1–4]. Most of the available analyses have been done in the frequency domain, including extensive results for the "exact" dissipative model [3,4]. For system level simulations and analytical studies of hydraulic systems, time domain solutions of the governing conservation equations are often desirable. For this purpose, modal approximation of the analytical frequency domain solutions offers an alternative technique to direct numerical solutions [5–7].

The one-dimensional distributed parameter model of a fluid transmission line, shown schematically in Fig. 1, can be expressed by the so-called four-pole equations that relate the upstream pressure p_u and flow rate q_u with the downstream pressure p_d and flow rate q_d expressed in the Laplace domain (Viersma [3]). The four pole equations can take one of four causal forms [2]. The modal approximations for two of the four causal forms have been treated by Yang and Tobler [6] and Van Schothorst [7]. Yang and Tobler considered the causal form with $[P_u(s)Q_d(s)]^T$ as input and $[P_d(s)Q_u(s)]^T$ as output while Van Schothorst dealt with the causal form with $[Q_u(s)Q_d(s)]^T$ as input and $[P_u(s)P_d(s)]^T$ as output. The third causal form with $[P_d(s)Q_u(s)]^T$ input and $[P_u(s)Q_d(s)]^T$ output can be obtained by switching the convention for the direction of the flow from the case treated by Yang and Tobler [6].

This technical brief deals with the fourth causality case with $[P_d(s)p_u(s)]^T$ input and $[Q_u(s)Q_d(s)]^T$ output for hydraulic transmission lines for which the linear friction model applies (those with small dissipation number). A typical application of this causality case is for modeling short connection lines to accumulators, which have been shown to be very important for hydraulic system dynamics by Versma [3]. Figure 2 shows the schematic of such a system, where a preferred integration causality assignment for the accumulator and the use of the first causality case from Ref. [6] for the sections of the main line, leads to the fourth case for the short connection line to the accumulator. The double-headed arrows in the figure indicate the input-output causality assigned to each line element.

In the rest of this technical brief, both transfer function and state space descriptions of the modal approximation for the fourth causality case are derived and simplifications are presented.

2 Transmission Line Model

The causal four-pole equation with upstream and downstream pressures as inputs and upstream and downstream flow rates as outputs has the following form:

$$\begin{bmatrix} Q_u(s) \\ Q_d(s) \end{bmatrix} = \begin{bmatrix} \dfrac{\cosh\Gamma(s)}{Z_c(s)\sinh\Gamma(s)} & -\dfrac{1}{Z_c(s)\sinh\Gamma(s)} \\ \dfrac{1}{Z_c(s)\sinh\Gamma(s)} & -\dfrac{\cosh\Gamma(s)}{Z_c(s)\sinh\Gamma(s)} \end{bmatrix} \begin{bmatrix} P_u(s) \\ P_d(s) \end{bmatrix} \quad (1)$$

The expressions for the line characteristic impedance $Z_c(s)$ and the propagation operator $\Gamma(s)$ depend on whether the basic model chosen is the lossless model, the linear friction model, or the dissipative model [2]. The linear friction case is considered here. Using the normalized Laplace operator $\bar{s}=s/\omega_c$, where $\omega_c=\nu/r_h^2$ is the viscosity frequency, the propagation operator $\Gamma(\bar{s})$, and the line characteristic impedance $Z_c(\bar{s})$ for the linear friction model are given, respectively, by

$$\Gamma(\bar{s}) = D_n\bar{s}\sqrt{1+\frac{8}{\bar{s}}}, \quad (2)$$

$$Z_c(\bar{s}) = Z_0\sqrt{1+\frac{8}{\bar{s}}} \quad (3)$$

The dissipation number D_n and the line impedance constant are given, respectively, by

$$D_n = \frac{l\nu}{cr_h^2}, \quad (4)$$

$$Z_0 = \frac{\rho c}{A} \quad (5)$$

where c is the speed of sound in the fluid given by

$$c = \sqrt{\frac{\beta_e}{\rho}} \quad (6)$$

The effective bulk modulus of the fluid β_e takes into account the flexibility of the wall of transmission line, compressibility of the fluid and also of any entrapped air.

In the following, the modal approximation for Eq. (1) is derived using a method similar to the one described in Ref. [6]. The goal is to represent each of the transcendental transfer functions in Eq. (1) as finite sum approximations of low-order polynomial transfer functions. To this end, the following result from Oldenburger and Goodson [9] is used:

$$\sinh\Gamma(\bar{s}) = \Gamma(\bar{s})\sum_{i=1}^{\infty}\left(1+\frac{\Gamma^2(\bar{s})}{D_n^2\lambda^2_{si}}\right), \quad (7)$$

where

$$\lambda_{si} = \frac{i\pi}{D_n}, \quad i = 1,2,3,\ldots \quad (8)$$

The approach is to use the result in Eq. (7) to find the poles of the individual transcendental transfer functions in Eq. (1) and then use

Contributed by the Dynamic Systems, Measurement, and Control Division of THE AMERICAN SOCIETY OF MECHANICAL ENGINEERS for publication in the ASME JOURNAL OF DYNAMIC SYSTEMS, MEASUREMENT, AND CONTROL. Manuscript received: April 7, 2004. Final manuscript revision received: September 18, 2004. Associate Editor: Noah Manring.

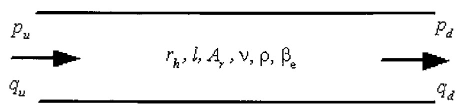

Fig. 1 One-dimensional fluid transmission line

partial fraction expansions to obtain the modal approximations. First, the zeroes of the transfer function $Z_c(\bar{s})\sinh\Gamma(\bar{s})$ are computed using Eqs. (2), (3), and (7)

$$Z_c(\bar{s})\sinh\Gamma(\bar{s}) = Z_0 D_n(\bar{s}+8)\prod_{i=1}^{\infty}\left(1+\frac{\Gamma^2}{D_n^2\lambda_{si}^2}\right)=0$$
$$\Leftrightarrow \bar{s}=-8 \vee \bar{s}=-4\pm\sqrt{16-\lambda_{si}^2},\quad i=1,2,3,\ldots \tag{9}$$

Note that these zeroes are the poles of the original transfer functions in Eq. (1) and at the pole $\bar{s}=-8$, $\Gamma(\bar{s})=0$, $\cosh\Gamma(\bar{s})=1$ and $\sinh\Gamma(\bar{s})=0$. At the pole pairs $\bar{s}=a_i\pm b_i=\bar{s}=-4\pm\sqrt{16-\lambda_{si}^2}$,

$$\cosh\Gamma(\bar{s})=\cosh(\pm jD_n\lambda_{si})=\cosh(\pm j\pi i)=\cos(\pi i)$$
$$=(-1)^i,\ i=1,2,3,\ldots.$$

Note that all of the poles are simple poles [8]. The general partial fraction expansion takes the form

$$f(\bar{s})=\frac{g(\bar{s})}{h(\bar{s})}=\frac{R_0}{\bar{s}+8}+\sum_{i=1}^{\infty}\left(\frac{R_i}{\bar{s}-(a_i+b_i)}+\frac{G_i}{\bar{s}-(a_i-b_i)}\right) \tag{10}$$

The coefficient R_0 can be computed using

$$R_0=\lim_{\bar{s}\to-8} f(\bar{s})(\bar{s}+8) \tag{11}$$

The coefficients R_i and G_i are better computed using residues since the numerator and denominator functions are analytic at the respective poles $\bar{s}=a_i\pm b_i$,

$$R_i,G_i=\mathrm{Re}\ s\{f(\bar{s})\}\Big|\bar{s}=a_i\pm b_i=\frac{g(\bar{s})}{h'(\bar{s})}\Big|\bar{s}=a_i\pm b_i \tag{12}$$

Once these residues are computed, the following observation applies:

$$\frac{A_i}{\bar{s}-(a_i+b_i)}+\frac{B_i}{\bar{s}-(a_i-b_i)}=\frac{(A_i+B_i)(\bar{s}-a_i)+(A_i-B_i)b_i}{(\bar{s}-a_i)^2-b_i^2} \tag{13}$$

The denominator in Eq. (13) simplifies to the quadratic $(\bar{s}^2+8\bar{s}+\lambda_{si}^2)$.

3 Modal Representation of $1/Z_c(\bar{s})\sinh\Gamma(\bar{s})$ and $\cosh\Gamma(\bar{s})/Z_c(\bar{s})\sinh\Gamma(\bar{s})$

The above-presented results will now be used to determine the modal representation for each of the two unique elements of the transfer matrix in Eq. (1). First, consider the element $f(\bar{s})=1/Z_c(\bar{s})\sinh\Gamma(\bar{s})$. Using Eqs. (2) and (3) in Eq. (11) together with the comments following Eq. (9), the coefficient R_0 is computed as

$$R_0=\lim_{\bar{s}\to-8}(s+8)\frac{1}{Z_0D_n(\bar{s}+8)\prod_{i=1}^{\infty}\left(1+\frac{\Gamma^2(\bar{s})}{D_n^2\lambda_{si}^2}\right)}=\frac{1}{Z_0D_n} \tag{14}$$

For the other coefficients, note that

$$\mathrm{Re}\ s\left\{\frac{1}{Z_c(\bar{s})\sinh\Gamma(\bar{s})}\right\}_{\bar{s}=a_i\pm b_i}=\left\{\frac{1}{Z_c'(\bar{s})\sinh\Gamma(\bar{s})+Z_c(\bar{s})\Gamma'(\bar{s})\cosh\Gamma(\bar{s})}\right\}_{\bar{s}=a_i\pm b}, \tag{15}$$

where it can be shown that

$$Z_c'(\bar{s})=\frac{-4Z_0}{\bar{s}^2\sqrt{1+\frac{8}{\bar{s}}}} \tag{16}$$

and

$$\Gamma'(\bar{s})=\frac{D_n^2}{\Gamma(\bar{s})}(\bar{s}+4) \tag{17}$$

Using Eqs. (2), (3), (16), and (17) and the notes following Eq. (9), Eq. (15) can be evaluated as

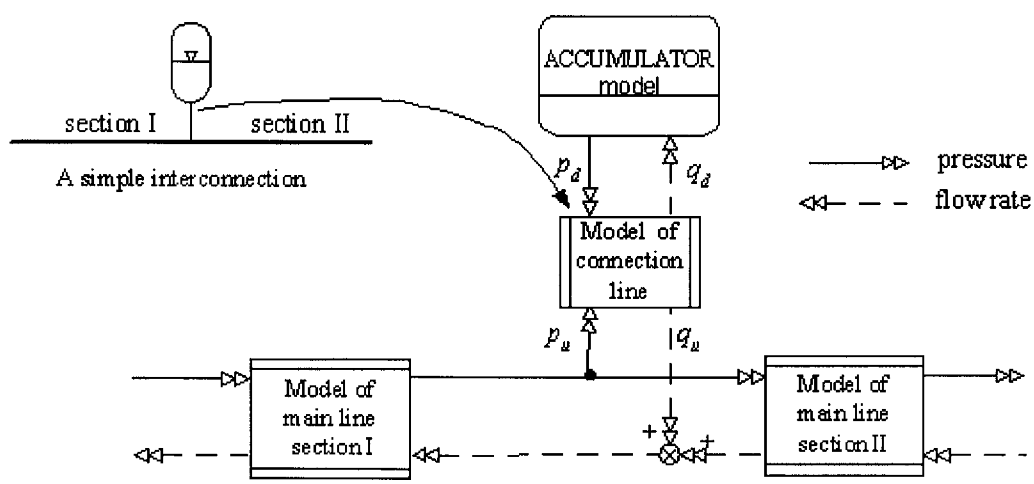

Fig. 2 Schematic of an application for the causality case considered here

$$R_i, G_i = \operatorname{Re} s\left\{\frac{1}{Z_c(\bar{s})\sinh\Gamma(\bar{s})}\right\}_{s=a_i\pm b_i} = \frac{-(1)^i(-4\pm\sqrt{16-\lambda_{si}^2})}{\pm Z_0 D_n\sqrt{16-\lambda_{si}^2}} \tag{18}$$

Substituting Eq. (18) into Eq. (13) and using the result together with Eq. (14) in Eq. (10), and simplifying the expression, the following modal representation results for $1/Z_c(\bar{s})\sinh\Gamma(\bar{s})$:

$$\frac{1}{Z_c(\bar{s})\sinh\Gamma(\bar{s})} = \frac{1}{Z_0 D_n}\left(\frac{1}{\bar{s}+8} + \sum_{i=1}^{\infty}\frac{(-1)^i 2\bar{s}}{\bar{s}^2+8\bar{s}+\lambda_{si}^2}\right) \tag{19}$$

For the other unique element of the transfer matrix $f(\bar{s}) = \cosh\Gamma(\bar{s})/Z_c(\bar{s})\sinh\Gamma(\bar{s})$, R_0 is computed as

$$R_0 = \lim_{\bar{s}\to -8}(\bar{s}+8)\frac{\cosh\Gamma(\bar{s})}{Z_0 D_n(\bar{s}+8)\prod_{i=1}^{\infty}\left(1+\frac{\Gamma^2(\bar{s})}{D_n^2\lambda_{si}^2}\right)} = \frac{1}{Z_0 D_n} \tag{20}$$

Using Eqs (2), (16), and (17), and the notes following Eq. (9)

$$\begin{aligned} R_i, G_i &= \operatorname{Re} s\left\{\frac{\cosh\Gamma(\bar{s})}{Z_c(\bar{s})\sinh\Gamma(\bar{s})}\right\}_{\bar{s}=a_i\pm b_i} \\ &= \left\{\frac{\cosh\Gamma(\bar{s})}{Z_c'(\bar{s})\sinh\Gamma(\bar{s}) + Z_c(\bar{s})\Gamma'(\bar{s})\cosh\Gamma(\bar{s})}\right\}_{\bar{s}=a_i\pm b_i} \\ &= \frac{-4\pm\sqrt{16-\lambda_{si}^2}}{\pm Z_0 D_n\sqrt{16-\lambda_{si}^2}} \end{aligned} \tag{21}$$

Finally, using Eq. (13) with R_i and G_i from Eq. (21) and substituting the result together with Eq. (20) into Eq. (10) and simplifying the expression, the modal representation for $\cosh\Gamma(\bar{s})/Z_c(\bar{s})\sinh\Gamma(\bar{s})$ results,

$$\frac{\cosh\Gamma(\bar{s})}{Z_c(\bar{s})\sinh\Gamma(\bar{s})} = \frac{1}{Z_0 D_n}\left(\frac{1}{\bar{s}+8} + \sum_{i=1}^{\infty}\frac{2\bar{s}}{\bar{s}^2+8\bar{s}+\lambda_{si}^2}\right) \tag{22}$$

4 Modal Approximation

Using Eqs. (19) and (22), the four-pole equation (1) can be re-written as

$$\begin{bmatrix} Q_u(\bar{s}) \\ Q_d(\bar{s}) \end{bmatrix} = \frac{1}{Z_0 D_n(\bar{s}+8)}\begin{bmatrix} 1 & -1 \\ 1 & -1 \end{bmatrix}\begin{bmatrix} P_u(\bar{s}) \\ P_d(\bar{s}) \end{bmatrix} + \frac{2\bar{s}}{Z_0 D_n(\bar{s}^2+8\bar{s}+\lambda_{si}^2)}\sum_{i=1}^{\infty}\begin{bmatrix} 1 & -(-1)^i \\ (-1)^i & -1 \end{bmatrix}\begin{bmatrix} P_u(\bar{s}) \\ P_d(\bar{s}) \end{bmatrix} \tag{23}$$

It should be noted that unlike the causality case treated in Ref. [6], where only quadratic terms appear in the modal representation, the case treated here contains a first-order lag term in addition to the quadratic modes. This will have an implication in the simplification of the final result.

The modal approximation is obtained by truncating the summation in Eq. (23) to a finite number of terms. Figure 3 shows a Bode plot for the element (1,1) of the exact transfer matrix given in Eq. (1), and the modal approximation taken from Eq. (23) with the first-order term only, the approximation with the first-order plus one second-order term and the approximation with the first-order plus two second-order terms included in the summation. Figure 4 shows the same information for element (2,1) of the transfer matrix given in Eq. (1). The overall number of terms to be included in the approximation depends on the application's frequency regime of interest.

It can be seen from Figs. 3 and 4 that for a wide range of normalized frequency (of the order of 10^4) the model given by Eq.

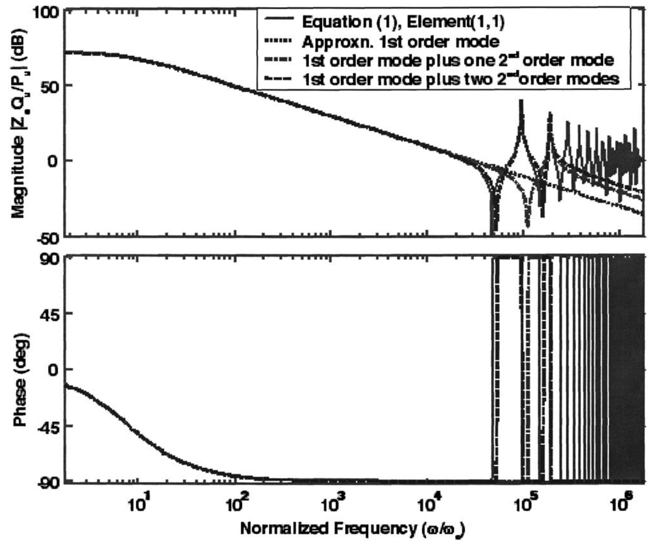

Fig. 3 Comparison of the modal approximation for element (1,1) in Eq. (1)

(1) can be approximated by the first-order lag term only. This observation implies that for a typical circular sectioned line with a fluid viscosity of 44 cSt and a line diameter of 3 cm, the line can be considered as a low-pass filter with a break frequency of about 2 Hz provided the overall frequency regime of interest for the application lies below 311 Hz. In this manner, the order of the system to which the transmission line belongs can be reduced significantly.

5 State Space Representation of the Modal Approximation

For time domain simulations, convenient state space forms can be derived for the approximation. Unlike the causality case treated by Van Schothorst [7], the block observer/observability canonical form does not lead to a minimum order realization for the causality case treated here. Instead, the following minimal state space formulation is derived by inspection from the modal transfer functions in Eq. (23):

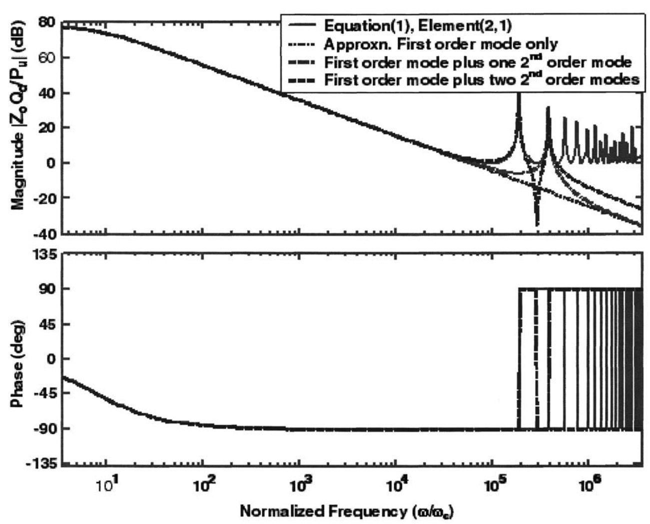

Fig. 4 Comparison of the modal approximation for element (2,1) in Eq. (1)

$$\frac{1}{\omega_c}\dot{\boldsymbol{x}}_i = \boldsymbol{A}_i\boldsymbol{x}_i + \boldsymbol{B}_i\boldsymbol{u}, \quad i = 0,1,2,3,\ldots, \tag{24}$$

$$\boldsymbol{y}_i = \boldsymbol{C}_i\boldsymbol{x}_i, \quad i = 0,1,2,3,\ldots \tag{25}$$

The input and the output vectors are

$$\boldsymbol{u} = \begin{bmatrix} p_u \\ p_d \end{bmatrix} \tag{26}$$

$$\boldsymbol{y} = \begin{bmatrix} q_u \\ q_d \end{bmatrix} = \sum_{n=1}^{n} \boldsymbol{y}_i = \sum_{n=1}^{n} \boldsymbol{C}_i\boldsymbol{x}_i \tag{27}$$

The coefficient matrices are, for the first-order mode ($i=0$)

$$\boldsymbol{A}_0 = \begin{bmatrix} -8 & 0 \\ 0 & -8 \end{bmatrix}, \quad \boldsymbol{B}_0 = \frac{1}{Z_0 D_n}\begin{bmatrix} 1 & -1 \\ 1 & -1 \end{bmatrix}, \quad \boldsymbol{C}_0 = \begin{bmatrix} 1 & 0 \\ 0 & 1 \end{bmatrix} \tag{28}$$

and for the second-order modes ($i=1,2,3,\ldots$)

$$\boldsymbol{A}_i = \begin{bmatrix} 0 & -\lambda_{si}^2 \\ 1 & -8 \end{bmatrix}, \quad \boldsymbol{B}_i = \frac{2}{Z_0 D_n}\begin{bmatrix} 0 & 0 \\ 1 & -(-1)^i \end{bmatrix}, \quad \boldsymbol{C}_i = \begin{bmatrix} 0 & 1 \\ 1 & (-1)^i \end{bmatrix} \tag{29}$$

For an n-mode approximation, the state equations can be augmented diagonally as follows:

$$\frac{1}{\omega_c}\dot{\boldsymbol{x}} = \boldsymbol{A}\boldsymbol{x} + \boldsymbol{B}\boldsymbol{u}, \tag{30}$$

$$\boldsymbol{y} = \boldsymbol{C}\boldsymbol{x}, \tag{31}$$

where the augmented state vector and the coefficient matrices are

$$x = [x_1 \; x_2 \; x_3 \; \cdots \; x_n]^T$$

$$\boldsymbol{A} = diag[\boldsymbol{A}_1 \; \boldsymbol{A}_2 \; \boldsymbol{A}_3 \; \cdots \; \boldsymbol{A}_n]$$

$$\boldsymbol{B} = [\boldsymbol{B}_1 \; \boldsymbol{B}_2 \; \boldsymbol{B}_3 \; \cdots \; \boldsymbol{B}_n]^T$$

$$\boldsymbol{C} = [\boldsymbol{C}_1 \; \boldsymbol{C}_2 \; \boldsymbol{C}_3 \; \cdots \; \boldsymbol{C}_n] \tag{32}$$

The modal state vectors $\boldsymbol{x}_i$ describing the second-order modes do not have a simple interpretation of partitioned (modal) output like the causality cases treated in Ref. [6,7] since the modal output matrices in Eq. (29) are not identity matrices. This should not cause any problems as long as the model is properly interfaced with connecting subsystems with the input and output vectors given above. It should also be noted that as long as the first-order mode is included in the approximation, the steady state value of the truncated approximation of Eq. (23) with a finite number of modes is the same as that of exact equation, Eq. (1). Unlike the causality cases treated in Refs. [6,7], there is no need to apply steady-state corrections to the approximation to offset the error of truncation. This implies that in hydraulic system modeling, whenever the causality assignment of the whole system permits it, the causality form given by Eq. (1) with the modal approximation given in this paper offers better handling of steady-state response.

The state space description chosen above for the first-order mode has a simple interpretation: the state variables are the partitioned (modal) outputs. For a range of normalized low frequency, the inclusion of only the first-order term in the approximation of Eq. (23) leads to the following relation for the upstream and downstream flow rates:

$$Q_u(s) = Q_d(s) = \frac{(P_u(s) - P_d(s))}{Ls + R} \tag{33}$$

where the L and R are the lumped inertance and resistance of the line given, respectively, by

$$L = \frac{\rho l}{A} \tag{34}$$

and

$$R = \frac{8\rho l v}{A_r r_h^2} \tag{35}$$

Therefore, for short connection lines or when $D_n < 0.001$ for which the linear friction model applies [6], the transmission line model given by Eq. (1) can be approximated by a simple series combination of the lumped hydraulic inertance and resistance. This result implies that any compressibility effects in the transmission line are neglected for the causality case given by Eq. (1) when a first-order approximation is used. When short connecting lines to gas charged or spring loaded hydraulic accumulators are modeled with this causality case, this result supports the usual assumption that the oil side compressibility is negligible compared to the gas/spring side.

6 Conclusion

In this paper, modal approximation methods are applied to one causality case of the four-pole equations for which the upstream and downstream pressures are inputs and the upstream and downstream flow rates are outputs. This causality case of the four-pole equations is applicable to hydraulic transmission lines with a small dissipation number, $D_n < 0.001$, for which the linear friction model is considered applicable. Both transfer function and state space models are given that can be directly incorporated into hydraulic system models. As long as the first-order mode is included in the approximation, no steady state correction measures are necessary to offset the error of truncation to a finite number of modes. It is also shown that for a wide range of frequencies the model can be represented by a first-order lag term containing only the series interconnection of the lumped hydraulic resistance and inertance of the line.

Nomenclature

A_r	=	cross-sectional area
$\boldsymbol{A}, \boldsymbol{B}, \boldsymbol{C}$	=	state, input and output matrices for augmented model
a_i, b_i	=	root components defined following Eq. (9)
$\boldsymbol{A}_i, \boldsymbol{B}_i, \boldsymbol{C}_i$	=	state, input and output matrices for ith mode
c	=	speed of sound
D_n	=	dissipation number
f, g, h	=	dummy functions of s or $\bar{S}$
i	=	integer mode index (i=0, *1,2,3,…*)
j	=	$\sqrt{-1}$ imaginary constant
l	=	length of line
L	=	line hydraulic inertance
p_w, p_d	=	upstream and downstream pressures in time domain
P_w, P_d	=	upstream and downstream pressures in Laplace domain
q_w, q_d	=	upstream and downstream flow rates in time domain
Q_u, Q_d	=	upstream and downstream flow rates in Laplace domain
R	=	line hydraulic resistance
r_h	=	hydraulic radius
R_i, G_i	=	residues in partial fraction expansion
s	=	Laplace operator
$\bar{s}$	=	normalized Laplace operator $\bar{s} = s/\omega_c$
$\boldsymbol{u}$	=	input vector defined by Eq. (26)
x	=	dummy variable
$\boldsymbol{x}$	=	state vector for augmented model
$\boldsymbol{x}_i$	=	modal state vector for ith mode
$\boldsymbol{y}$	=	output vector defined by Eq. (27)

$\boldsymbol{y}_i$ = output vector for ith mode
Z_0 = line impedance constant
Z_c = line characteristic impedance
β_e = effective bulk modulus
Γ = propagation operator
λ_{si} = root indices defined by Eq. (8)
ρ = density
ν = kinematic viscosity
ω_c = viscosity frequency $\omega_c = \nu / r_h^2$
ω = frequency in rad/s

References

[1] D'Souza, A.F., and Oldenburger, R., 1964, "Dynamic Response of Fluid Lines," J. Basic Eng., **86**, pp. 589–598.

[2] Goodson, R. E., and Leonard, R. G., 1972, "A Survey of Modeling Techniques for Fluid Line Transients," J. Basic Eng., **94**, pp. 474–482.

[3] Viersma, T. J., 1980, *Analysis, Synthesis and Design of Hydraulic Servosystems and Pipelines*, Studies in Mechanical Engineering I, Elsevier, Amsterdam, The Netherlands.

[4] Woods, R. L., Hsu, C. H., and Chung, C. H., 1983, "Comparison of Theoretical and Experimental Fluid Line Responses With Source and Load Impedance," *Fluid Transmission Line Dynamics*, M. E. Franke and T. M. Drzewiecki, eds., ASME Special Publications, New York, pp. 1–36.

[5] Hsue, C. Y.-Y., and Hullender, D. A, 1983, "Modal Approximations for the Fluid Dynamics of Hydraulic and Pneumatic Transmission Lines," *Fluid Transmission Line Dynamics*, M. E. Franke and T. M. Drzewiecki, eds., ASME Special Publication, New York, pp. 51–77.

[6] Yang, W. C., and Tobler, W. E., 1991, "Dissipative Modal Approximation of Fluid Transmission Lines Using Linear Friction Model," Trans. ASME, J. Dyn. Syst. Meas., **113**, pp. 152–162.

[7] Van Schothorst, G., 1997, "Modeling of Long-Stroke Hydraulic Servo-Systems for Flight Simulator Motion Control and System Design," Ph.D. thesis, Delft University of Technology, The Netherlands.

[8] Kreyszig, E., 1999, *Advanced Engineering Mathematics*, 8th Ed., Wiley New York.

[9] Oldenburger, R., and Goodson, R. E., 1964, "Simplification of Hydraulic Line Dynamics by Use of Infinite Products," J. Basic Eng., **86**, pp. 1–10.